Direct Imaging of Molecular Transport Through Skin

Erik R. Scott, J. Bradley Phipps,* and Henry S. White†

Medtronic, Inc., Brooklyn Center, Minnesota; *Alza Corporation, Spring Lake Park, Minnesota; and †Department of Chemistry, University of Utah, Salt Lake City, Utah, U.S.A.

Scanning electrochemical microscopy (SECM) was used to image spatial variations in the molecular flux of $Fe(CN)_6^{-4}$ across excised hairless and nude mouse skin. The SECM response is specific to electroactive molecules, allowing selective imaging of the flux of $Fe(CN)_6^{-4}$ in multicomponent ionic solutions. Quantitative SECM image analysis demonstrated that 40% to 60% of the total $Fe(CN)_6^{-4}$ flux occurred through appendages in the skin. SECM analysis of skin samples exposed to a known transport enhancer, sodium dodecylsulfate, indicated that the increase in the ion transport rate occurred exclusively in nonporous skin tissue. ***J Invest Dermatol 104:142–145, 1995***

The medical community recently has focused increased attention on administering drugs at a continuously controlled rate, to optimize therapeutic treatment [1]. One means of achieving controlled release is by molecular transport across the skin, commonly referred to as transdermal drug delivery (TDD). TDD systems are either passive, in which a molecular species diffuses across the skin along a concentration gradient; or active, in which an external field, such as an electric potential gradient, is applied to facilitate permeation. In either case, drug molecules enter the lower layers of the skin and are transported throughout the body by the circulatory system.

A fundamental question in TDD is the extent to which molecular transport occurs through appendages in the skin, such as hair follicles and sweat ducts. It is generally accepted that such appendages provide low-resistance pathways across the stratum corneum. Although many qualitative studies have shown enhanced flux of species near appendages [2–5], it has proved difficult to measure the absolute rate of transport of a molecular species through individual skin appendages.

In this report, we describe measurements of the magnitude of molecular transport rates across skin using scanning electrochemical microscopy (SECM). Originally developed for characterization of electrochemical processes [6,7] SECM also has proved useful for imaging localized molecular fluxes through synthetic and biologic porous membranes [8,9]. In particular, relatively simple analyses of SECM images allow one to determine the absolute rates of molecular transport [9] through individual pores. This capability makes possible quantitative analysis of the distribution of current across biologic membranes, such as skin. In this study, we report SECM imaging and quantitative analysis of molecular transport across mouse skin. The effects of a transport enhancer, sodium dodecylsulfate (SDS), on the current distribution of ionic species across skin are quantified using SECM.

Manuscript received April 26, 1994; revised August 2, 1994; accepted for publication September 5, 1994.

Reprint requests to: Dr. Henry S. White, Department of Chemistry, Henry Eyring Building, University of Utah, Salt lake City, UT 84112.

Abbreviations: SECM, scanning electrochemical microscope; TDD, transdermal drug delivery.

MATERIALS AND METHODS

All chemicals were used as received and were A.C.S. reagent grade or higher. Water (18 MΩ) was purified using either a Water Prodigy System (Labconco, Kansas City, MO) or E Pure System (Barnestad, Dubuque, IA).

Skin was removed from the back and sides of freshly sacrificed hairless mice (male, ages 7–12 weeks, Charles River, strain SKH-1) and nude mice (male, ages 28–31 weeks, Charles River, strain CD1-nu-nu). The loosely attached subcutaneous fat was removed gently with a damp gauze sponge. Mouse skin samples were placed between layers of sterile saline-soaked gauze in a plastic bag and stored in a refrigerator until use. Storage times ranged from 4 to 32 h. No correlation was found between the duration of storage and either the overall transport or the pore transport rates. Disk-shaped areas of skin (0.50 cm^2)were exposed to solution.

The SECM imaging system that we have constructed **(Fig 1)** consists of a diffusion cell in which the donor and receptor compartments are separated by a skin sample. A detailed description of the instrument and its operation has been given elsewhere [9]. The donor solution contains an electroactive species, such as $Fe(CN)_6^{-4}$, which is driven across the sample by a current applied between the two Ag/AgCl electrodes. (The current density, j_{app}, across the skin sample is defined as the applied current divided by the exposed area of the skin sample.) As $Fe(CN)_6^{-4}$ emerges from the skin, it is detected on the receptor side of the skin using a microelectrode probe that is rastered across the skin surface [9]. The current at the microelectrode is proportional to the local concentration of $Fe(CN)_6^{-4}$ through the faradaic reaction, $Fe(CN)_6^{-4} \rightarrow Fe(CN)_6^{-3} + e^-$, which occurs at a mass-transport–limited rate at the electrode surface. Spatial variations in the concentration of $Fe(CN)_6^{-4}$ are detected as variations in the faradaic current at the microelectrode tip and serve to determine directly those regions in the skin where the $Fe(CN)_6^{-4}$ flux is large. The relation between the faradaic current measured at the tip and the local concentration of $Fe(CN)_6^{-4}$, at a position defined by the spatial coordinates x, y, and z, is given by the following [9]:

$$i_t = 2\pi nFDC(x,y,z)r_t. \quad (1)$$

In equation 1, n is the number of electrons transferred per molecule (=1), D is the diffusion constant of $Fe(CN)_6^{-4}$ (0.65×10^{-5} cm^2/second), F is Faraday's constant (96,484 coulomb/eq) and r_t is the radius of the microelectrode tip (4 μm).

0022-202X/95/$09.50 • SSDI0022-202X(94)00271-8

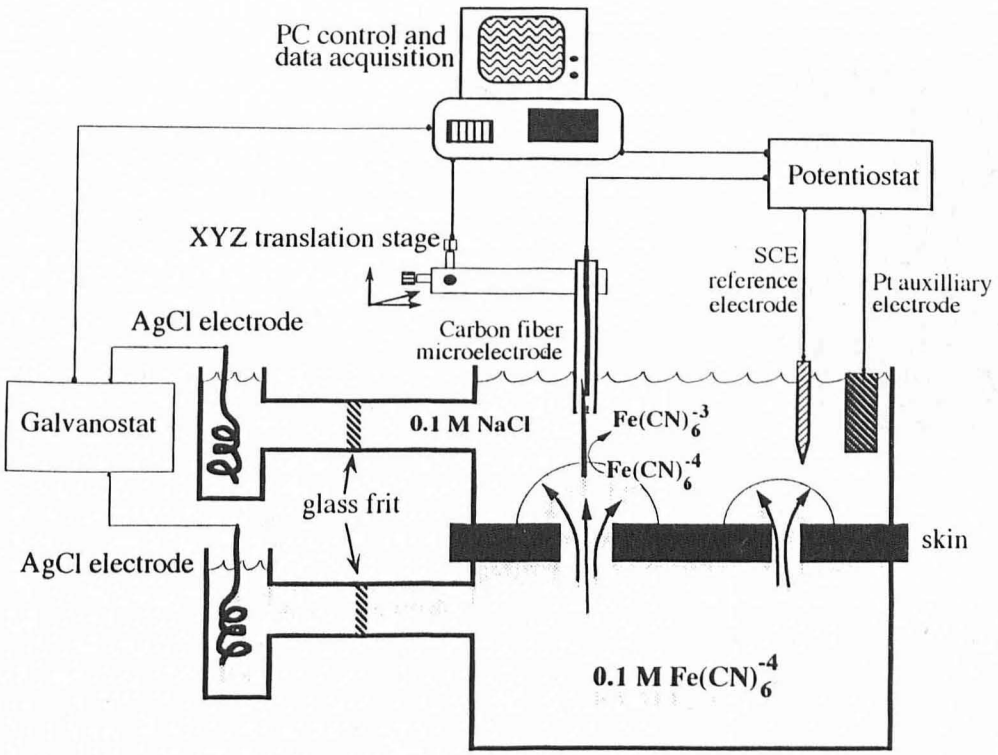

Figure 1. Schematic representation of the scanning electrochemical microscope used for imaging molecular transport across skin. The carbon fiber microelectrode is insulated with poly(phenyleneoxide) except at the very end. The two Ag/AgCl electrodes drive the current across the skin sample (area = 0.5 cm^2).

RESULTS AND DISCUSSION

Figure 2*A* shows a typical SECM image of hairless mouse skin obtained at an applied current density, j_{app} of 40 $\mu A/cm^2$. In these experiments, the donor solution contained 0.1 M $K_4Fe(CN)_6$, and the receptor compartment contained either 0.1 M NaCl or a phosphate-buffered saline solution composed of 0.1 M NaCl with 50 mM H_2KPO_4/HK_2PO_4 (pH 7.28). Despite their names, the skins of hairless and nude mice have an abundance of hair follicles (most of which contain no hair shafts [10]). We have shown recently that these structures provide pathways for ion transport [9,11]. The two bright regions of the SECM image shown in **Fig 2*A*** correspond to high local concentrations of $Fe(CN)_6^{-4}$, indicating a large flux of $Fe(CN)_6^{-4}$ through localized regions in the skin sample. We refer to such transport-active sites as "pores," without regard to their exact physiologic identity. We also refer to transport that occurs through pathways other than these pores as "nonporous" or "homogeneous" transport. Using a dye-staining technique [11], the number of active current-carrying pores previously has been shown to be a function of j_{app} and time. At current densities commonly used in clinical TDD practice (50–200 $\mu A/cm^2$), the number of pores approaches a quasi–steady-state value after approximately 30 min of iontophoresis [9–12]. From SECM images of mouse skin, we estimate a pore density of approximately 130 pores/cm^2 at j_{app} = 40 $\mu A/cm^2$, in good agreement with previous estimates determined at the same current density using the staining technique. **Table I** summarizes typical experimental conditions and the pore densities for hairless and nude mouse skin samples measured using SECM.

The absolute rate of transport of $Fe(CN)_6^{-4}$ through an individual pore is determined by measuring the faradaic current at the SECM microelectrode tip, i_t, at different vertical heights above the skin, z, while rastering the microelectrode in the x,y plane. The local concentration of $Fe(CN)_6^{-4}$, C (x,y,z), is calculated from the values of i_t using equation 1; isoconcentration lines that connect points in space, where C (x,y,z) is constant, are plotted from the data set. Because the pores in skin have microscopic dimensions, the flux of $Fe(CN)_6^{-4}$ from the pores is radially divergent and results in hemisphere-shaped isoconcentration surfaces [9], as shown for a pore in **Fig 2*B***. The radius of the hemispheric isoconcentration line (r_{hs}) is obtained by a least-squares fit to the data. The steady-state rate of mass transport N_p (mol/second) of $Fe(CN)_6^{-4}$ through the pore is then calculated using equation 2 from the unique values of r_{hs} and C(x,y,z) that define the hemispheric isoconcentration line [9]:

$$J_p = 2\pi DC(x,y,z)r_{hs}. \quad (2)$$

Values of J_p determined for individual pores ranged from 0.011 to 0.69 $\times$ 10^{-12} mol/second. Some pores had transport rates less than this, but values of J_p could not be extracted reliably for them, because of a low signal-to-noise ratio. Overall, greater than 75% of all pores that were detectable by SECM had sufficient transport rates to be analyzed quantitatively by the above method.

The transport rates for individual pores (J_p) were summed according to equation 3 to yield the total transport rate (J_{sum}) of $Fe(CN)_6^{-4}$ through all pores in each skin sample:

$$J_{sum} = \Sigma J_p. \quad (3)$$

The number of pores surveyed and pore densities are given in **Table I**. The overall rate of $Fe(CN)_6^{-4}$ transport across the skin (J_{tot}), through both porous and nonporous paths, also was determined quantitatively by analysis of the Fe concentration in the receptor-compartment solution after passage of current for periods ranging from 3 to 20 h. Fe was analyzed using either inductively coupled plasma-mass spectroscopy or atomic adsorption spectroscopy (calibration standards were 0.1 M NaCl solutions containing 0 to 40 ppm K_4 $Fe(CN)_6$). Values of J_{sum} and J_{tot} are listed in **Table I**.

The fraction of $Fe(CN)_6^{-4}$ transport that occurs through pores is given directly by the ratio of J_{sum} and J_{tot}:

$$f_p = J_{sum}/J_{tot}. \quad (4)$$

For the four hairless mouse samples studied, values of f_p ranged from 0.34 to 0.66, with an average value of 0.47 $\pm$ 0.16 (**Table I**).

J_{sum} and J_{tot} also were measured for four nude mouse samples at current densities ranging from 10 to 40 $\mu A/cm^2$and are reported in **Table I**. Values of f_p ranged from 0.08 to 0.67. The significant variation in the values of f_p for nude mice may attest to an increased

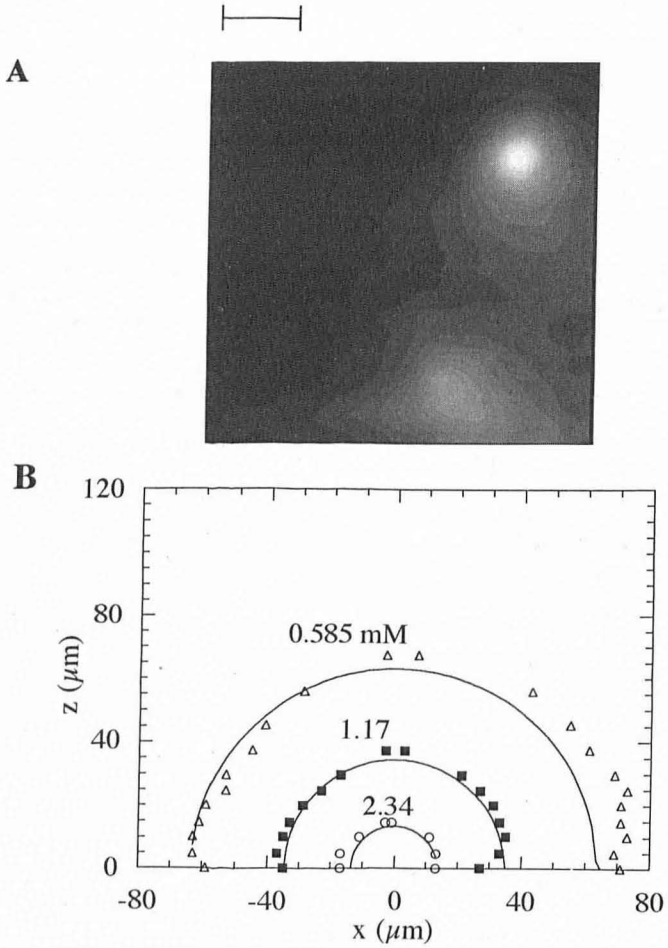

Figure 2. SECM image and isoconcentration lines. *A*) SECM image of a 1000 × 1000-μm area of hairless mouse skin at j_{app} = 40 μA/cm^2. The two bright areas correspond to locally high concentrations of $Fe(CN)_6^{-4}$. Donor solution: 0.1 M $K_4Fe(CN)_6^{-4}$; receptor solution: 0.1 M NaCl. *Scale bar*: 200 μm. *B*) Isoconcentration lines above a pore. The concentration of $Fe(CN)_6^{-4}$ corresponding to each isoconcentration line is given on the figure. The least-squares semicircular fits to the data are shown as *solid lines*.

site-to-site variability in the density of pores relative to hairless mice.

Exposure of skin to SDS increases skin permeability to water and other substances, especially at SDS concentrations above the critical micelle concentration of 8 mM. It has been theorized that this effect results from an interaction of the surfactant with proteins in the stratum corneum [13,14]. We explored this hypothesis using the SECM analysis of pore transport described above.

Table II. Effect of SDS Treatment on Pore Transport for Hairless Mouse Skin

t_{sds}[a] (min)	Sample	j_{app} (μA/cm^2)	ΔJ_{tot}[b] (%)	ΔJ_{sum}[c]	Δf_p[d]
10	4	40	+8%	−1%	−8%
20	1	40	+29%	−1%	−23%
30	2	40	+132%	−20%	−65%

[a] Duration of exposure to 50 mM SDS solution.
[b] Relative change in overall transport rate of $Fe(CN)_6^{-4}$ after SDS exposure.
[c] Relative change in the transport of $Fe(CN)_6^{-4}$ through pores after SDS exposure.
[d] Relative change in the fraction of transport through pores.

Solutions used to study the effect of surfactant treatment of skin were prepared by adding SDS to the NaCl or the phosphate-buffered saline receptor solution such that the SDS concentration was 50 mM, well above the critical micelle concentration for SDS (8 mM [15]). After initially determining the total pore transport rate, J_{sum}, we replaced the receptor solution with the SDS solution for times ranging from 10 to 30 min. During this period, the applied current was turned off. After the skin was exposed to the SDS solution, the receptor compartment was rinsed five times and refilled with the original receptor solution (phosphate-buffered saline or NaCl). Current was again applied, and SECM was then used to remeasure the pore transport rates over the same sample areas as those studied before the SDS treatment. Because of the time required to measure the pore transport rates, the average total time elapsed between the before- and after-SDS measurements of pore transport was approximately 3 h.

Table II summarizes variations in the pore transport rate and the overall transport rate before and after SDS treatment. SDS treatment resulted in an 8% to 132% increase in the overall (porous and nonporous) transport of $Fe(CN)_6^{-4}$, J_{tot}, consistent with the expectation that SDS increases the permeability of skin. In addition, the relative increase in J_{tot} correlated well with the length of exposure of the skin sample to the SDS solution. However, when current is delivered from a constant current source, the net ion transport rate across the sample is constant. Therefore, it is not necessary or even expected that an increase in skin permeability results in an increase in J_{tot} for $Fe(CN)_6^{-4}$ or any other ion. In this constant-current experiment, the increase in J_{tot} results either from an increase in the relative mobility of $Fe(CN)_6^{-4}$ (compared to other ions within the skin) or from an increase in the non-iontophoretic (diffusional and convective) component of $Fe(CN)_6^{-4}$ transport. It is not clear from our measurements which of these two phenomena is taking place. However, the interesting result of these experiments is that the SDS-induced increase in the overall transport rate of $Fe(CN)_6^{-4}$ was not associated with the pores, even though

Table I. Transport Parameters for Hairless and Nude Mouse Skin

Skin Type	Sample Number	Receptor Solution[a]	j_{app}[b] (μA/cm^2)	Area Surveyed (cm^2)	Number of Pores Measured	Density of Pores (n_p; cm^{-2})	Pore Transport Rate ($J_{sum} \times 10^{13}$; mol/s)	Overal Transport Rate ($J_{tot} \times 10^{13}$; mol/s)	Fractional Pore Transport[c] (f_p)
Hairless mouse	1	PBS	40	0.05	5	100	4.24	12.1	0.35
	2	PBS	40	0.04	6	150	5.66	8.57	0.66
	3	PBS	19	0.04	4	100	1.20	3.53	0.34
	4	NaCl	40	0.02	3	150	2.11	3.91	0.54
Nude mouse	5	NaCl	10	0.10	8	80	1.04	2.53	0.41
	6	NaCl	20	0.06	4	67	3.05	10.9	0.28
	7a	NaCl	20	0.09	3	33	1.98	24.75	0.08
	7b	NaCl	20	0.09	3	33	3.18	26.5	0.12
	8	NaCl	40	0.04	7	175	15.5	23.1	0.67

[a] PBS, phosphate-buffered saline (0.1 M NaCl, 50 mM Na_2HPO_4/NaH_2PO_4, pH 7.28); NaCl, 0.1 M NaCl.
[b] Applied current passed between the Ag/AgCl electrodes (see **Fig 1**).
[c] Fractional pore transport, $f_p = J_{sum}/J_{tot}$.

approximately 50% of the total transport of $Fe(CN)_6^{-4}$ occurs through pores. In fact, SDS exposure resulted in a decrease in the rate of transport of $Fe(CN)_6^{-4}$ through pores, J_{sum} **(Table II)**. SECM imaging of the skin before and after SDS treatment revealed that no new pores were formed as a result of the treatment.

Changes in the fractional contribution of pores to the total transport rate as a result of the SDS treatment, denoted in **Table II** as Δf_p, were approximately equal and opposite to changes in J_{tot}. This observation is consistent with a model by which enhancement of the overall transport occurs through the "homogeneous" (nonporous) tissue. We conclude that the enhancement effect of SDS results from interaction of the surfactant with structures that make up the nonporous tissue, such as the keratin of corneocytes or the intercellular lipid matrix.

These experiments demonstrate the power of SECM not only as an imaging instrument, but also as an analytical tool capable of measuring quantitatively mass-transport phenomena in complex biologic systems.

REFERENCES

1. Langer H: New methods of drug delivery. *Science* 249:1527–1533, 1990
2. Cullander C, Guy RH: Sites of iontophoretic current flow into the skin: identification and characterization with the vibrating probe electrode. *J Invest Dermatol* 97:55–64, 1991
3. Burnette R, Ongipipattanakul B: Characterization of the pore transport properties and tissue alteration of excised human skin during iontophoresis. *J Pharm Sci* 77:132–137, 1988
4. Grimnes S: Pathways of ionic flow through human skin in vivo. *Acta Dermatol Venereol (Stockh)* 64:93–98, 1984
5. Abramson HA, Engel MG: Skin reactions. XII. Patterns produced in the skin by electrophoresis of dyes. *Arch Dermatol Syph* 44:190–200, 1941
6. Bard AJ, Fan F-RF, Pierce DT, Unwin PR, Wipf DO, Zhou F: Chemical imaging of surfaces with the scanning electrochemical microscope. *Science* 254:68–73, 1991
7. Engstrom RC, Pharr CM: Scanning electrochemical microscopy. *Anal Chem* 61:1099A–1104A, 1989
8. Scott ER, White HS, Phipps JB: Scanning electrochemical microscopy of a porous membrane. *J Membrane Sci* 58:71–87, 1991
9. Scott ER, White HS, Phipps JB: Iontophoretic transport through porous membranes using scanning electrochemical microscopy: application to in vitro studies of ion fluxes through skin. *Anal Chem* 65:1537, 1993
10. Köpf-Maier P, Mboneko VF, Merker HJ: Nude mice are not hairless. *Acta Anat* 139:178–190, 1990
11. Scott ER, White HS, Phipps JB: Transport of ionic species in skin: contribution of pores to the overall skin conductance. *Pharm Res* 10:1699–1709, 1993
12. Burnette RR, Ongipipattanakul B: Characterization of the permselective properties of excised human skin during iontophoresis. *J Pharm Sci* 76:765–773, 1987
13. Cooper ER, Berner B: In: Rieger MM (ed.). *Surfactants in Cosmetics*. Marcel Dekker, New York, 1985, pp 195–210
14. Blank IH, Gould E: Permeation of anionic surfactants (surface active agents) into skin. *J Invest Dermatol* 33:327–336, 1959
15. Rhein LD, Robbins CR, Fernee K, Cantore R: Surfactant structure effects on swelling of isolated human stratum corneum. *J Soc Cosmet Chem* 37:125–139, 1986